20th Australasian Fluid Mechanics Conference
Perth, Australia
5-8 December 2016

Propagation of Internal Tides on the Northwest Australian Shelf Studied with Time-Augmented Empirical Orthogonal Functions

J. W. Book[1], N. L. Jones[2], R. J. Lowe[2], G. N. Ivey[2], C. R. Steinberg[3], R. M. Brinkman[3], A. E. Rice[1], C. E. Bluteau[2], S. R. Smith[1], T. A. Smith[1], and S. Matt[1]

[1]Oceanography Division, U.S. Naval Research Laboratory, Stennis Space Center, Mississippi 39529, USA

[2]School of Civil, Environmental and Mining Engineering & Oceans Institute, University of Western Australia, Crawley, Western Australia 6009, Australia

[3]Australian Institute of Marine Science, Townsville, Queensland 4810, Australia

Abstract

A series of collaborations between U.S. and Australian funded projects resulted in the deployment of 30 moorings at 23 different sites between November 2011 and August 2012 along the Northwest Australian Shelf (NWS), a region of strong internal tide oscillations. The measurement program peaked during April 2012.

A time-augmented empirical orthogonal function (EOF) technique was developed and implemented that allowed the correlated variability, structure, and phasing of semidiurnal internal tide packets to be evaluated at multiple mooring sites. This technique allows the EOF analysis to preserve the non-linear character of the internal wave packets without requiring a large number of EOF modes.

In three different examples from the NWS, between 45% and 65% of the variance of complex internal tide dominated temperature structures were explained using only two EOF modes. Using only the first mode of the EOFs our analysis also identified a propagation blocking effect that was found to be associated with the mesoscale coastal circulation and the wind.

Introduction

The Northwest Australian Shelf (NWS) is an area well known for the presence of large-amplitude internal tide generated wave packets [7, 8, 6, 1]. With respect to the southwestern portion of this shelf, most research has been focused on a particular section near Dampier that aligns with the North West Shelf Venture, Australia's largest hydrocarbons project. However, in 2011/2012 a collaboration between the U.S. Naval Research Laboratory, the University of Western Australia, and the Australian Institute of Marine Science led to a wider instrumentation of the southwest section of the shelf including the deployment of 30 moorings at 23 different locations (see Figure 1) with many of these specifically set up to sample internal tide wave packets.

The moorings were divided into four observational clusters or Nodes that were each designed to resolve both the along-shore and cross-shore internal tide wave structure at that location. Having four Nodes spread along the shelf allowed for study of the impact of both stronger and weaker tidal forcing on internal tide propagation, as the M_2 barotropic tidal energy flux varied from a low value of 4 kW/m in Node 1 to a high value of 36 kW/m in Node 4. Also, the impact of shelf topography could be studied as Nodes 1 and 3 have a steep shelf/slope profile while Nodes 2 and 4 are less steep.

In this paper, we will focus on only the six moorings marked in purple and labeled in Figure 1. Each of these moorings were sub-surface taut line moorings with buoyancy pulling upward

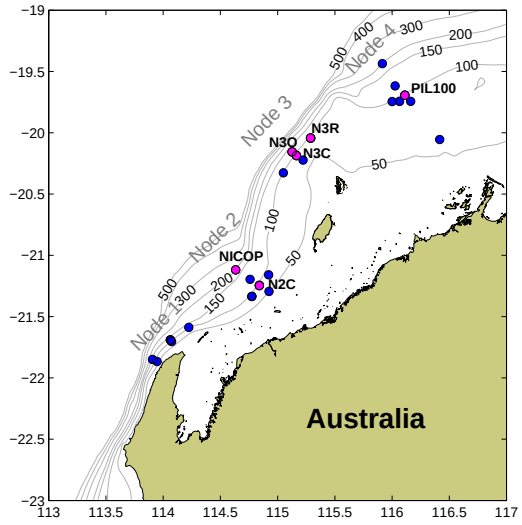

Figure 1: Map of moorings (blue and purple circles) deployed in 2011/2012 and distributed to form four separate nodes of concentrated observations on the NWS. The 50 m, 100 m, 150 m, 200 m, 300 m, 400 m, and 500 m isobath contours are drawn in gray. Moorings featured in this paper are colored purple.

on a wire against an anchor to suspend sensors in the water column at selected depth intervals. The suspended sensors consisted of Sea-Bird Electronics MicroCATs to measure temperature and conductivity, and VEMCO Minilog II-T sensors to measure only temperature. Some MicroCATs were equipped to also measure pressure, and the NICOP and PIL100 moorings additionally had Acoustic Doppler Current Profilers (ADCPs) suspended on the wire. ADCPs were also deployed next to the other four moorings in separate trawl-resistant bottom mounts. N2C, N3C, N3R, and PIL100 were all deployed along the 100 m isobath, N2O was deployed on the 120 m isobath, and NICOP was deployed on the 200 m isobath. The temperature time series measured at these moorings are analyzed in this paper to study how the internal tide packets generated at the offshore slope propagate and evolve at various places along the shelf.

Empirical orthogonal functions (EOFs) are a powerful tool for analyzing multiple time-series records. EOFs allow the records to be objectively mapped to new orthogonal basis functions that describe the maximum variance of the set of records in descending order from the first basis function to the last basis function. Thus, most of the variance is carried by the first few basis functions (or modes) and basis functions that carry little variance can be safely neglected for many analyses. In this process, empirical connections are revealed between the original records

by how they combine into the new basis functions to describe variances that are common to separate records. However, conventional EOFs are not well suited for analysis of all types of variance. They combine variability over all frequency bands and have difficulty in describing progressive wave features [4] which can pose challenges if the dataset contains propagating waves with specific frequencies.

In this paper, we examine signals of propagating non-linear internal tide packets on the NWS. These non-linear features are not easily analyzed by either conventional EOFs or spectral variations of EOF methodology [4] because the signals are non-stationary and have correlated variability across multiple frequencies. Overall, we seek to determine the space-time structure of the wave packets as they propagate and evolve between multiple observational moorings as well as to determine how these wave packets evolve over multiple weeks of tidal cycles.

Some past efforts of analyzing internal tide structure with EOFs included: merging two mooring datasets close to each other with time-evolving EOFs and an objective function fitting procedure [10], computing standard EOFs and analyzing the time amplitudes with regards to tidal frequencies [2], and solving for empirical patterns in EOF time amplitudes over tidal cycles [3]. However, these methods use various assumptions that are not well suited for the internal tide packets of the NWS, such as assuming that the packets are stationary between moorings, or stationary over multiple tidal cycles, or can be represented with a few dominant frequencies.

Methodology

In this paper, we develop a slightly modified form of an extended EOF analysis [14, 5, 13, 9] to make it more applicable to the specific case of non-linear internal wave packets generated by the internal tide cycle. An extended EOF analysis analyzes together all spatially separated observations at a given point in time with all spatially separated observations at a given number of additional time points in either delayed or advanced time steps or both. Thus specified time delays/advances are treated as if they are additional spatially separated observations and the resulting EOFs have information about these time delays included in their spatial modes. Our methodology follows [5] by having a continuous window of time delays treated together (see their Figure 4), but with the important exception that we do not slide our window in time. We instead advance it by one window length for each time point, thereby not allowing any time point in the series to be analyzed in more than one window time. Thus we are augmenting space in the EOF analysis with the time evolution of the variables over a short time window.

For a single line mooring measuring temperature time series at different ocean depths, this time-augmented EOF procedure reduces the problem to be essentially the same as applying a standard EOF analysis to a time series of geographic spatial maps of temperature [11] except that depth variations act as latitude variations and time variations within the window act as longitude variations in this analogy. Figure 2 shows an example of the procedure used to break apart a set of temperature time series at different depths (top panel) into a 36 member (two example members shown in the bottom panels) long time series of tidal cycle maps (our time-augmentation window is chosen to align with the 12.4 period cycle of the dominate M_2 tides) with the x axis variable being time progression within the tidal cycle, τ, and the y axis variable being depth below sea level, z.

An EOF analysis was then applied to the 36 member time series of tidal cycle blocks by singular value decomposition [4],

$$A = USV^T \tag{1}$$

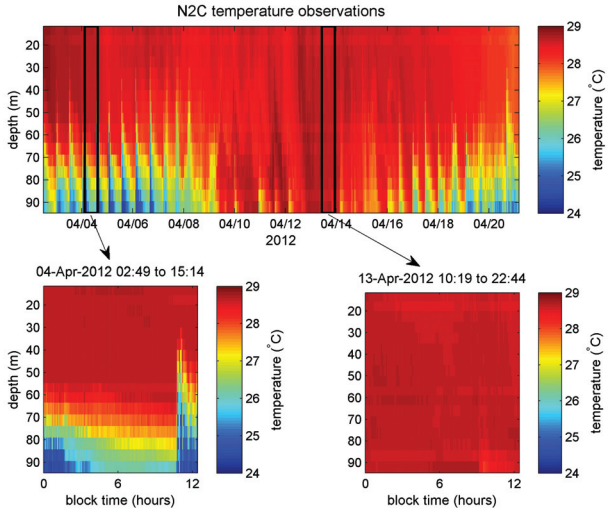

Figure 2: Top panel shows the temperature (color) recorded at 17 discrete ocean depths from mooring N2C (see Figure 1) from April 2-21, 2012. The black boxes mark two separate examples of 12.42 hour time blocks within the longer time series. Bottom panels show these two example time blocks. Altogether the top panel is broken into 36 time blocks (only two are shown here) that span the total record with no overlap in time.

$$\begin{bmatrix} T'(z_1,\tau_1,t_1) & T'(z_1,\tau_1,t_2) & \dots \\ T'(z_2,\tau_1,t_1) & \dots & \dots \\ \dots & \dots & \dots \\ T'(z_1,\tau_2,t_1) & \dots & \dots \\ \dots & \dots & \dots \end{bmatrix} = \begin{bmatrix} M_1(z_1,\tau_1) & M_2(z_1,\tau_1) & \dots \\ M_1(z_2,\tau_1) & \dots & \dots \\ \dots & \dots & \dots \\ M_1(z_1,\tau_2) & \dots & \dots \\ \dots & \dots & \dots \end{bmatrix} \begin{bmatrix} \lambda_1 & 0 & \dots \\ 0 & \lambda_2 & \dots \\ 0 & 0 & \dots \\ \dots & \dots & \dots \end{bmatrix} V^T \tag{2}$$

with the A matrix being composed of the temperature anomalies, T', with each column having all the anomaly values for a given tidal cycle block at all z levels and τ times ranging from 0 to 12.42 hours. Each column is offset in time from its neighbor by the 12.42 hour time step associated with the tidal cycle time variable, t. The time average that was removed in forming T' was the average over t for all values of z and τ. The EOF represents temperature variations in z and τ from an average packet structure in a tidal cycle. In the singular value decomposition, the EOF modal structures, M are the columns of the U matrix, the relative variance explained by each mode is given by λ^2, and the EOF time amplitudes are the rows of the matrix SV^T. In the rest of the paper, for display purposes, each U matrix is multiplied by the absolute maximum time amplitude value of mode 1 and the time amplitudes are normalized by the same value.

This method can be extended to include the temperatures observed at separate mooring sites by just concatenating additional A matrices associated with each additional mooring site below the first one. The computed EOF modes and time amplitudes from the larger A matrix will now be ranked according to the dominate modes of variance across all the mooring sites, allowing for analysis of propagation and evolution of packet structure from site to site.

Results

Figure 3 shows the results of applying this methodology us-

ing the N2C mooring data shown in Figure 2 together with the NICOP mooring data from farther offshore (Figure 1). The observed average internal tide packet structure at both sites showed a wave like structure with oscillations near the bottom at site N2C and at mid-water column depth at site NICOP. EOF modes 1 and 2 account for 46.4% and 17.2% of the variance from these means, respectively. The EOF mode 1 structure for N2C is very close to an exact negative of the mean structure. Thus when the time amplitude for this mode (Figure 4) is highly positive, this mode can serve to cancel the mean wave structure and represent times when the wave packet does not propagate to this site. Indeed this is exactly what is happening from April 9-15 (see Figure 4 and the bottom-right panel of Figure 2 for an example on April 13th). In contrast, the EOF mode 1 structure for NICOP is not a negative field of the mean structure. This reflects the fact that the internal tide packets did not disappear during the April 9-15 period at the 200 m isobath location in Node 2. The disappearance of the wave packet at N2C was not in phase with the tidal neap cycle as spring tides peaked on April 9th at this location.

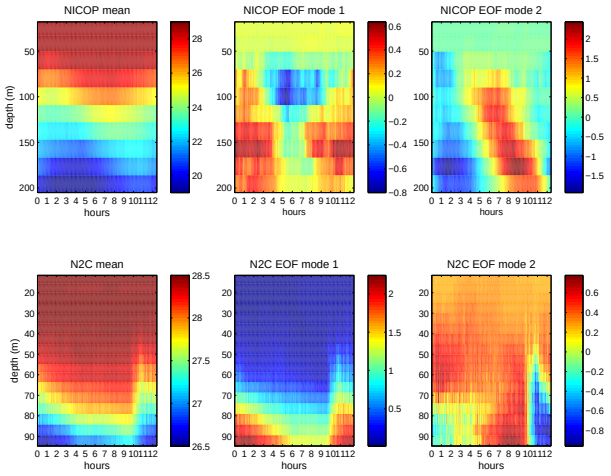

Figure 3: Left-hand panels are the deployment time-average internal tide packet temperature structures in z and τ for Node 2 moorings N2C and NICOP. Center panels are mode 1 EOF temperature-anomaly structures in z and τ and right-hand panels are mode 2 EOF structures. EOF structures are all multiplied by the absolute maximum time amplitude value of mode 1 to better show the magnitude of the anomalies. Color bar units are $^{\circ}$C.

Figure 5 shows the results of performing the same analysis but for three moorings in Node 3. In this case, EOF mode 1 explains 55.1% of the variance and EOF mode 2 explains 10.0% of the variance. Just as was the case for N2C at Node 2, the EOF mode 1 structures look similar to negative fields of the mean structures. When this mode peaked around April 14th and 15th, internal tide packets (not shown) were absent at N3R, barely evident at N3C, and suppressed at N3O. An autonomous underwater vehicle glider was sampling further offshore during these dates and did observe internal tide packets. The general trend of the time amplitude for mode 1 (Figure 4) matches that of mode 1 for Node 2 suggesting that a similar dynamic is controlling suppression of inshore wave propagation at both Nodes.

This was further investigated using nine of the moorings shown in Figure 1 that were in place for five months on the NWS and it was found that the blocking of internal wave packet propagation from April 9-15 coincided with relaxation of mean northwestward winds and strengthening of a southwestward coastal current. The cross-shore pycnocline tilt upwards toward the coast between NICOP and N2C that is associated with the baroclinic

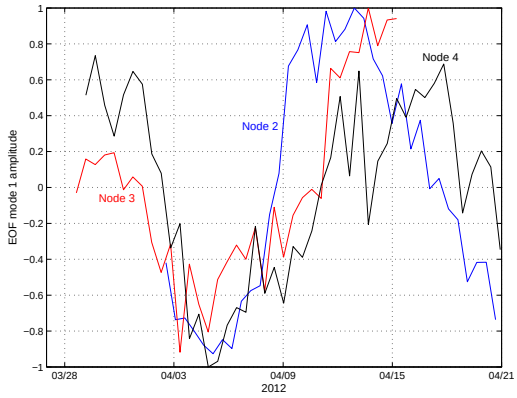

Figure 4: EOF mode 1 amplitude variations in time for Node 2 moorings (blue), Node 3 moorings (red), and the PIL100 mooring in Node 4 (black). Amplitudes are normalized by the respective absolute maximum values.

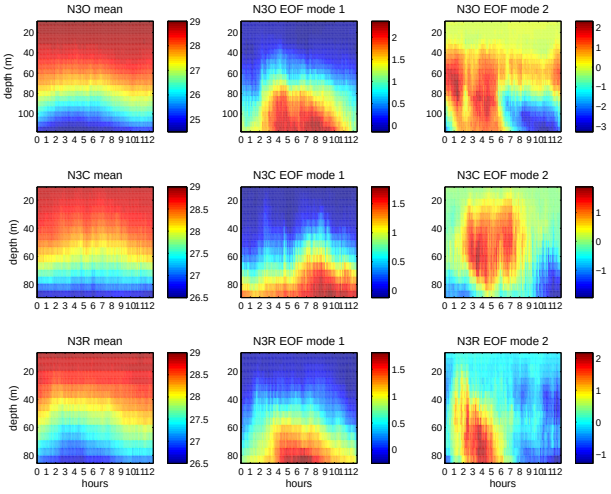

Figure 5: As in Figure 3, but for Node 3 moorings N3O, N3C, and N3R.

coastal current reversed its tilt on April 9th exactly when the wave packets stopped arriving at N2C. Whether this is due to stratification being eroded from downwelling winds or a more complex interaction between the waves and the coastal current [12] needs to be further investigated.

Node 4 moorings are near the North West Shelf Venture and from the past studies conducted there it is known that the wave packet structure is particularly complex in the region (e.g., see [6]). Therefore, we applied the time-augmented EOF methodology to the data from the PIL100 mooring located there (Figure 6). In this case, EOF mode 1 was less dominant explaining only 29.8% of the variance, with modes 2, 3, and 4 (not shown) explaining 14.7%, 12.3%, and 6.9% respectively. This is an indication of the complexity of the wave packet structures in Node 4. In addition, the mode 1 structure does not represent a wave packet cancelling mode as it did for the other 100 m isobath locations in Nodes 2 and 3. Instead it represents a phase shifting mode as can be commonly found in some extended EOF analyses [5]. For instance, adding 0.75 times the EOF mode 1 structure in Figure 6 to the mean will shift the occurrence of the wave peak (maximum isothermal displacement) to around $\tau = 4$ hours and subtracting 0.75 times EOF mode 1 from the mean will shift the occurrence of the wave peak to

around $\tau = 9$ hours. Figure 4 shows that such shifts were realized in the observed record.

A surprising finding was that although EOF mode 1 for Node 4 has a very different character than the EOF modes for Nodes 2 and 3, its time amplitude tracks the time amplitudes of the mode 1s from Nodes 2 and 3 remarkably well (Figure 4). These variations were found to be associated with the reversing coastal current and the wind field for Nodes 2 and 3, suggesting that phase-shifting of the wave packets for Node 4 could also be related to the coastal current variation and/or winds. The phase speeds of the packets are of the same order of magnitude [6] as the coastal current speeds, so phase-shifting interactions are at least plausible. Further investigation is warranted.

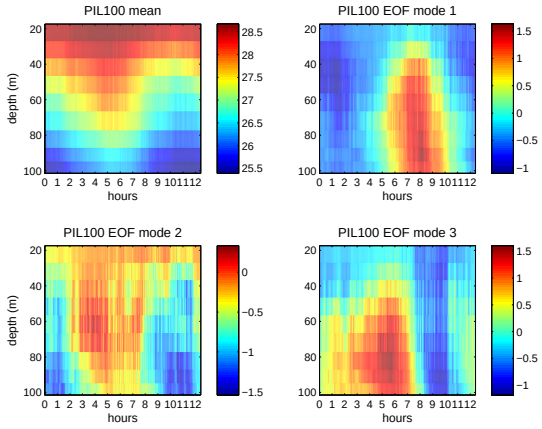

Figure 6: As in Figure 3, but for average and first 3 modes for the PIL100 mooring in Node 4.

Conclusions

Using two moorings in a relatively broader portion of the NWS study area, 64% of the internal tide wave packet variance was explained with just two EOF modes. Using three moorings in the topographically steepest portion of the NWS study area, two EOF modes explained 65% of the variance. In both these cases, the dominant EOF mode is related to changes brought on by a change in the mesoscale coastal current circulation and the cross-shore pycnocline tilt. Thus the NWS-wide wind and mesoscale circulation were directly impacting internal tide propagation. In a different area with more complex internal tide packets, three EOF modes explained only 58% of the variance, but mode 1 (which in this case acted to phase shift the wave packets) was again implied to be associated with wind and mesoscale circulation. These examples illustrate how this time-augmented EOF technique can be used to study the character of internal tide propagation onto a coastal shelf.

Acknowledgements

The Office of Naval Research (ONR) funded this work through the project “Propagation and Dissipation of Internal Tides on Coastal Shelves”. Additional funding was contributed by an Australian Research Council (ARC) Discovery Projects (DP 140101322), an ARC Linkage Project (LP 110100017), an ONR Naval International Cooperative Opportunities Project (N62909-11-1-7058), and an ONR funded project, “AUV Data Analysis for Predictability in Time-Evolving Regimes”. This work was also facilitated by an Institute of Advanced Studies Distinguished Visiting Fellowship awarded by the University of Western Australia. The PIL100 data was from the Integrated Marine Observing System (IMOS) – IMOS is a national collaborative research infrastructure, supported by the Australian Government. Thanks to Dr. Max Yaremchuk. Last but not least, we thank the science team and crew of the R/V Solander.

References

[1] Bluteau, C. E., Jones, N. L. and Ivey, G. N., Dynamics of a tidally-forced stratified shear flow on the continental slope, *Journal of Geophysical Research*, **116**.

[2] Bruno, M., Vázquez, A., Gómez-Enri, J., Vargas, J. M., García Lafuente, J., Ruiz-Cañavate, A., Mariscal, L. and Vidal, J., Observations of internal waves and associated mixing phenomena in the Portimao Canyon area, *Deep-Sea Research II*, **53**, 2006, 1219–1240.

[3] Casagrande, G., Stéphan, Y., Warn Varnas, A. C. and Folegot, T., A novel empirical orthogonal function (EOF)-based methodology to study the internal wave effects on acoustic propagation, *IEEE Journal of Oceanic Engineering*, **36**, 2011, 745–759.

[4] Emery, W. J. and Thomson, R. E., *Data Analysis Methods in Physical Oceanography*, Elsevier, New York, 2001, 2nd edition.

[5] Fraedrich, K., Pawson, S. and Wang, R., An EOF analysis of the vertical-time delay structure of the quasi-biennial oscillation, *Journal of the Atmospheric Sciences*, **50**, 1993, 3357–3365.

[6] Gastel, P. V., Ivey, G. N., Meuleners, M. J., Antenucci, J. P. and Fringer, O., The variability of the large-amplitude internal wave field on the Australian North West Shelf, *Continental Shelf Research*, **29**, 2009, 1373–1383.

[7] Holloway, P. E., Internal tides on the Australian North-West Shelf: A preliminary investigation, *Journal of Physical Oceanography*, **13**, 1983, 1357–1370.

[8] Holloway, P. E., Chatwin, P. G. and Craig, P., Internal tide observation from the Australian North West Shelf in summer 1995, *Journal of Physical Oceanography*, **31**, 2001, 1182–1199.

[9] Jacobs, G. A., Book, J. W., Perkins, H. T. and Teague, W. J., Inertial oscillations in the Korea Strait, *Journal of Geophysical Research*, **106**, 2001, 26943–26957.

[10] Lin, Y.-T., Newhall, A. E., Duda, T. F., Lermusiaux, P. F. J. and Haley, P. J., Merging multiple-partial-depth data time series using objective emperical orthogonal function fitting, *IEEE Journal of Oceanic Engineering*, **35**, 2010, 710–721.

[11] Messié, M. and Chavez, F., Global modes of sea surface temperature variability in relation to regional climate indices, *Journal of Climate*, **24**, 2011, 4314–4331.

[12] Mooers, C. N. K., Several effects of a baroclinic current on the cross-stream propagation of inertial-internal waves, *Geophysical Fluid Dynamics*, **6**, 1975, 245–275.

[13] Wang, R., Fraedrich, K. and Pawson, S., Phase-space characteristics of the tropical stratospheric quasi-biennial oscillation, *Journal of the Atmospheric Sciences*, **52**, 1995, 4482–4500.

[14] Weare, B. C. and Nasstrom, J. S., Examples of extended empirical orthogonal function analysis, *Monthly Weather Review*, **110**, 1982, 481–485.